ACS APPLIED MATERIALS & INTERFACES

Letter

www.acsami.org

Tailored Design of Architecturally Controlled Pt Nanoparticles with Huge Surface Areas toward Superior Unsupported Pt Electrocatalysts

Liang Wang,[†] Masataka Imura,[†] and Yusuke Yamauchi*[,†,‡,§]

[†]World Premier International (WPI) Research Center, International Center for Materials Nanoarchitectonics (MANA), National Institute for Materials Science (NIMS), Tsukuba 305-0044, Japan

[‡]PRESTO, Japan Science and Technology Agency (JST), Kawaguchi 332-0012, Japan

[§]Faculty of Science and Engineering, Waseda University, 3-4-1 Okubo, Shinjuku, Tokyo 169-8555, Japan

Supporting Information

ABSTRACT: Herein, we report a very simple and rapid method to synthesize two types of Pt nanoparticles with open porous structures (i.e., Pt nanodendrites and multiarmed Pt nanostars) in high yield. The present synthesis is performed by a simple sonication treatment of an aqueous solution containing K_2PtCl_4 and a nonionic block copolymer with branched alkyl chains in the presence of ascorbic acid (AA) at room temperature. Nanodendrites and multiarmed nanostars with different Pt nanostructures are selectively synthesized by simply controlling the dissolved block copolymer amounts in the reactive system. As-prepared 3D Pt nanodendrites and multiarmed Pt nanostars with well-defined morphologies are highly porous and self-supported structures assembled by staggered nanoarms as building blocks, thereby realizing extremely high surface areas (around 80 m^2 g^{-1}). The present synthesis has a remarkable advantage in its simplicity for the synthesis of Pt nanocatalysts, in comparison with other previous approaches. Our Pt nanodendrites and Pt nanostars not only improve the active Pt surface area but also show superior electrochemical performance, which make them promising electrocatalysts for future.

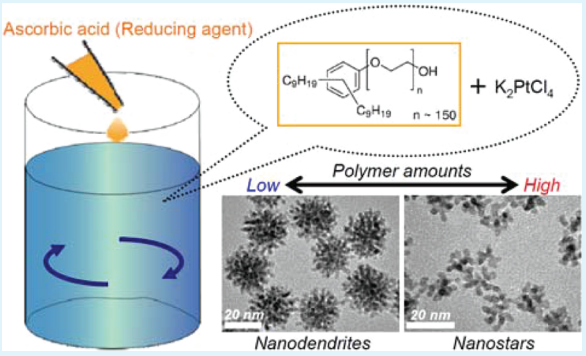

KEYWORDS: *Pt nanoparticle, electrocatalyst, chemical reduction, nanoporous structure, high surface area, ascorbic acid*

The shape- and size-controlled synthesis of Pt nanostructures is imperative in order to create highly active Pt catalysts (for instance, electrocatalysts for a methanol oxidation reaction (MOR) in a direct methanol fuel cell) at low cost.[1−5] The catalytic activities of Pt nanostructures can be tuned by tailoring their shapes and sizes.[6−11] Two distinct demonstrations are Pt nanocubes with concaved surfaces exhibiting higher catalytic activity for the oxygen reduction reaction (ORR) than Pt cubes with smooth exteriors,[12] and Pt cubic nanoboxes showed enhanced performance in MOR referenced to hollow Pt spheres.[13] The synthesis of active Pt nanocatalysts with desired shapes and sizes (e.g., nanoworms,[14] nanoraspberries,[15] nanocages,[16] nanowires,[17a−c] nanocubes,[17d] mesoporous films,[17e,f] and others[18−20]) is becoming increasingly important.

Among various Pt shapes, three-dimensional (3D) porous Pt nanostructures with their advantageous high surface area and high accessibility represent a highly promising type of catalyst. 3D nanoporous frameworks highly favor the desired "high mass specific activity" of the very rare and expensive Pt catalysts. In general, the template approach is a universal route to create a porous Pt nanoskeleton from the original confined nanospace followed by removal of the internal mold. In the hard-templating strategies,[21] mesoporous silica (e.g., MCM-48 and KIT-6) can be used as an efficient mold to synthesize ordered Pt replica structures.[22] In soft-template routes, lyotropic liquid crystals (LLCs) made of highly concentrated nonionic surfactants (or block copolymers)[23] are versatile soft-templates for the synthesis of ordered mesoporous Pt structures.[24] The template approaches provide predetermined the final porous Pt structures; however, the synthesis system is still complicated. Rational synthesis of porous Pt catalysts by a simpler and scalable route in large quantity still remains a significant challenge.

Currently, Pt nanocatalysts with highly dendritic morphologies have attracted considerable attention.[25−28] However, it is generally difficult to achieve spontaneous formation of highly anisotropic Pt nanodendrites, mainly because of the fact that Pt itself has an inherently highly symmetric face-centered cubic (fcc) crystal nature.[29] It is noteworthy that the previously reported routes are highly dependent on the selected synthetic conditions and/or multistep synthesis. For instance, Pt nanodendrites were prepared by reducing $Pt(acac)_2$ at a given high concentration by H_2 in organic solvents after 500 min, and a low concentration of $Pt(acac)_2$ led to irregular Pt nanostructures;[30] Pt nanodendrites were synthesized by

Received: April 5, 2012
Accepted: May 30, 2012
Published: June 6, 2012

multistep thermal decomposition of Pt precursors in organic solvent in the presence of hexadecylamine (HDA).[31] Consequently, "shape- and size-controlled synthesis" of Pt nanostructures is still a quite challenging issue.

Herein, we report a very simple and rapid method to synthesize two types of Pt nanoparticles with open porous structures (i.e., Pt nanodendrites and multiarmed Pt nanostars) in high yield (Figure 1 and Figure S1 in the Supporting

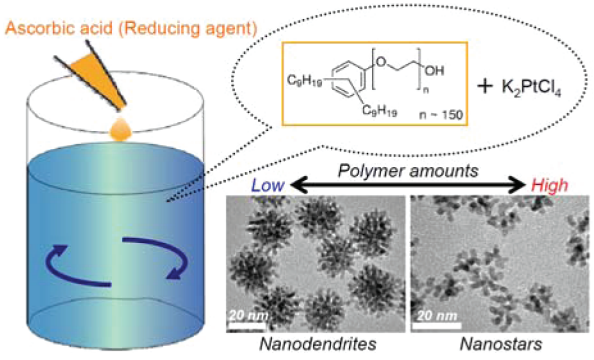

Figure 1. Schematic presentation for formation of Pt nanodendrites and Pt multiarmed nanostars. Different Pt nanostructures are selectively synthesized by simply controlling the dissolved block copolymer amounts in the reactive system. Enlarged image is shown in Figure S1 in the Supporting Information.

Information). The present synthesis was performed by a simple sonication treatment of an aqueous solution containing K_2PtCl_4 and a nonionic block copolymer with branched alkyl chains (the chemical structure is shown in Figure 1) in the presence of ascorbic acid (AA) at room temperature. Nanodendrites and multiarmed nanostars with different Pt nanostructures were selectively synthesized by simply controlling the dissolved block copolymer amounts in the reactive system (Figure 1). As-prepared 3D Pt nanodendrites and multiarmed Pt nanostars with well-defined morphologies are highly porous and self-supported structures assembled by staggered nanoarms as building blocks, thereby realizing extremely high surface areas (around 80 $m^2\ g^{-1}$).

The obtained Pt nanodendrites showed highly monodispersed 3D branched structures (Figure 2). Their particle size distribution was very narrow from 23 to 30 nm with a dominating diameter of around 26 nm (see Figure S2a in the Supporting Information). Careful observation confirmed that the Pt nanodendrites were assembled by staggered nanoarms with 2 nm in width as building blocks. The observed lattice fringes in each arm were assignable to the (111) plane of a Pt fcc structure, because the observed *d*-spacing was 0.23 nm (Inset image of Figure 2a). The random nanoarms fabricate deep nanocavities in each particle. The nanocaved structural feature is also clearly visualized by a high-angle annular dark-field scanning TEM (HAADF-STEM) observation (Figure 2b-2 and Figures S3a in the Supporting Information). Both the energy-dispersive X-ray (EDX) mapping and its spectrum indicated that the nanodendrites were composed of pure Pt (see Figure S4 in the Supporting Information). Several peaks for wide-angle X-ray diffraction (XRD) pattern could be assigned to be Pt fcc crystal nature (see Figure S5a in the Supporting Information), which is consistent with the selected area electron diffraction (ED) pattern (Inset image of Figure 2a).

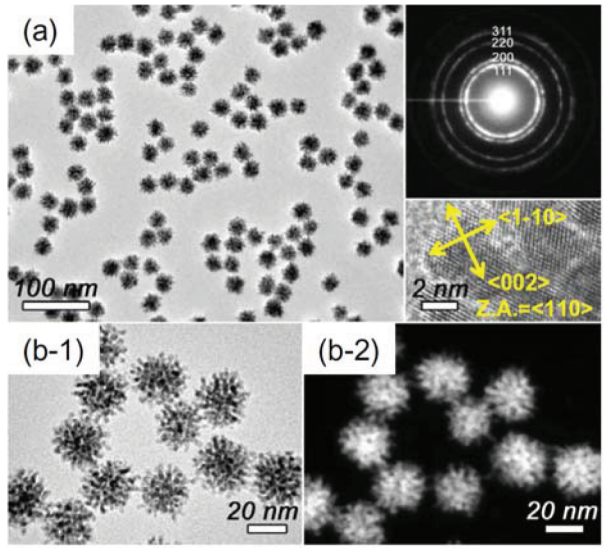

Figure 2. (a) TEM image of Pt nanodendrites at low magnification. Two inset images are selected-area ED pattern recorded from several particles and crystalline lattice fringes observed on the particle edge. b-2 is HAADF-STEM image of the same part of b-1.

Creating deep cavities with open porous structure in each Pt nanoparticle is of great importance to dramatically increase Pt-specific surface area. The present synthetic route is readily scaled up to afford a sufficient quantity of product for N_2 adsorption−desorption analysis (see Figure S6a in the Supporting Information). The as-prepared Pt nanodendrites showed an ultrahigh specific surface area of 77 $m^2\ g^{-1}$, which is much higher than all the existent unsupported Pt catalysts to the best of our knowledge. Among the previous papers, Pt dendritic nanoparticles (with 56 $m^2\ g^{-1}$)[5b] have been known as unsupported Pt catalysts with very high surface areas. For comparison, a commercial Pt catalyst (generally referred to as Pt black) has a surface area ranging from 20 to 28 $m^2\ g^{-1}$. Porous Pt nanoparticles and porous Pt nanoballs reported previously showed surface areas of 14[28] and 23 $m^2\ g^{-1}$,[18c] respectively.

The particle size presented here (averaging around 26 nm) was much smaller than those of the Pt nanodendrites reported previously.[26−28,31,32] Therefore, it is considered that the combination of the decreased particle size and the caved nanoarchitectures greatly increases the specific surface area of our Pt nanodendrites. Furthermore, another advantage in the Pt nanodendrites is inherent 3D self-supported constructions, which not only favor guest accessibility but also afford good tolerance to undesirable agglomeration of the active sites in catalytic reactions.[33]

Compared to the previous synthetic methods, there are several advantageous points in our process: (1) a remarkable simple reaction (one-step and one-pot synthesis at room temperature in an aqueous solution), (2) a very rapid reaction (within 5 min, which is the most rapid method so far), and (3) an ultrahigh surface area (around 80 $m^2\ g^{-1}$, which is comparable to all the existing unsupported Pt catalysts). This study is the first to explore the use of nonionic block copolymer polyoxyethylene dinonylphenyl ether with branched structures for synthesis of Pt nanostructures. The nonionic block copolymer used in this study is a commercially available and highly economical one. These advantages indicate that our

synthesis has the potential to make a significant contribution toward the syntheses of new Pt nanocatalysts.

To help understand the shape evolution of the Pt nanodendrites in the present reaction system, intermediate samples have been followed by TEM observation. As shown in Figure S7 in the Supporting Information, the Pt nanodendrites initially grew from a primary bumped particle. The bumped particle continuously grew in its main branches and new secondary branches to further form the final nanodendrites. At around 3 min, the color of the reaction solution remained opaque black in a stable manner, suggesting that the Pt precursor was completely reduced and mature structures of the nanoparticles had been obtained.

A high concentration of the Pt precursor is a key factor for the formation of the Pt nanodendrites. Pt precursor concentrations ranging from 15 mM to 20 mM (Figure 2 and Figure S8a in the Supporting Information) favor the dendritic growth of Pt structures in the investigated system, while a low Pt precursor concentration leads to Pt nanoparticles in an ill-defined form (see Figure S8b in the Supporting Information). A sufficient Pt precursor affords a rich Pt atomic addition, favoring the epitaxial growth of the bumped particles to highly branched Pt structures. On the other hand, an insufficient Pt source leads to the lack of free Pt atoms for overgrowth, most likely resulting in Pt irregular structures.

Significantly, by simply increasing the used amount of the nonionic block copolymer to 0.10 g in the reactive system, unique multiarmed Pt nanostars with an ultrahigh surface area of 72 $m^2 g^{-1}$ is successfully achieved at a 100% yield (Figure 3 and Figures S3b and S6b in the Supporting Information). The size of the multiarmed Pt nanostars narrowly ranges from 11 to 17 nm with an average diameter of around 14 nm (see Figure S2b in the Supporting Information). The XRD pattern of the multiarmed Pt nanostars is for randomly oriented fcc Pt crystals (see Figure S5b in the Supporting Information). The lattice fringes are coherently extended over the entire nanostars (Figure 3b). Each Pt nanostar is a single-crystalline nature, implying that the Pt arm is caused by continuous Pt atomic addition rather than by random aggregation of small Pt particles.[34] Importantly, several atomic kinks and steps derived from low-coordinated atoms were exposed on the arm exterior (as indicated by arrows in Figure 3c), which are of highly catalytic sites.[11,35,36] The Pt nanoarms were spatially separated from each other. Multiarmed Pt nanostars with nanoscale spatially and locally separated Pt arms favor the drastic suppression of the activity loss derived from the agglomeration of Pt active sites. This multiarmed Pt nanostar is a very recently discovered new type of structure and is a highly exciting catalyst.[34] To date, only few reports on the synthesis of multiarmed Pt nanostars have been published. As a recent significant achievement, multiarmed Pt nanostars were successfully obtained by a two-step seed-mediated growth strategy using tetrahedral Pt nanocrystals as seeds to direct the subsequent formation of multiarmed Pt nanostars via refluxing for 3 h at a boiling temperature.[34] In contrast, our synthetic approach is performed in the absence of any seed within 5 min at room temperature, making it quite different from the previous seeded growth method. Moreover, the obtained multiarmed Pt nanostars are strikingly uniform in both particle size and shape, which is also notably different from the reported ones prepared by seeded growth.[34]

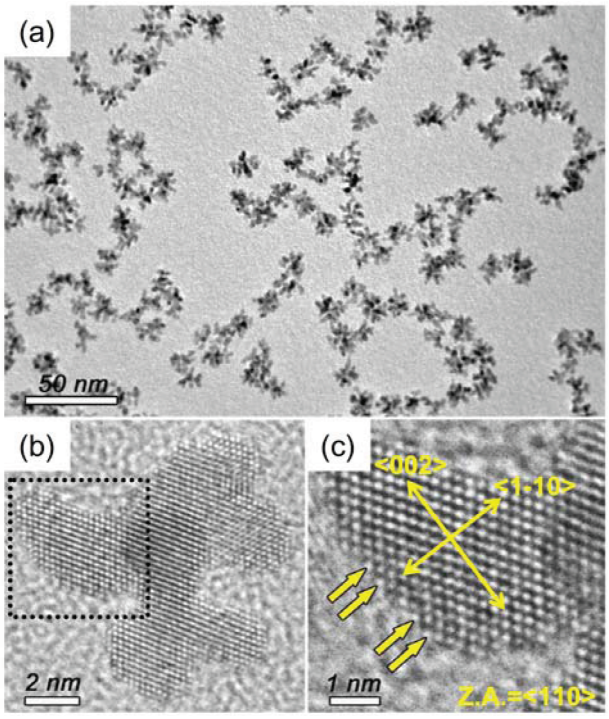

Figure 3. (a, b) TEM images of Pt nanostars at different magnifications. (c) Index of the lattice fringes observed on the square area of b. The atomic steps are indicated by the arrows.

As-prepared Pt nanodendrites and Pt nanostars are promising catalysts. Their electrocatalytic performance for MOR has been tested and further benchmarked against commercially available Pt black (see Figure S9 in the Supporting Information). Two obvious anodic peaks, which are typical features of the methanol oxidation process, are observed on all the three samples during the positive and negative sweeps in cyclic voltammogram (CV) investigations (see Figure S9a in the Supporting Information). The mass normalized current densities are 0.59, 0.52, and 0.11 A mg^{-1} for Pt nanostars, Pt nanodendrites and commercially available Pt black, respectively, in the positive direction sweep. The current densities of the Pt nanostars and Pt nanodendrites are 5.4 and 4.7 times higher than that of the Pt black and are also much higher than those of recent state-of-the-art supported Pt nanocatalysts such as Pt nanoparticles supported on carbon nanotubes (CNTs) (Pt/CNTs), PtRu nanoparticles supported on CNTs (PtRu/CNTs), Pt/CNTs/ionic liquid polymer (PIL) hybrids (Pt/CNTs-PIL), PtRu/CNTs/PIL hybrids (PtRu/CNTs-PIL),[37] Pt Nanowires supported on Sn@CNTs nanocable (PtNW-Sn@CNTs) and commercial ETEK Pt/C catalyst (30 wt % Pt) (see Figure S9d in the Supporting Information).[38] The value of I_f/I_b (in which I_f and I_b are the forward and backward current densities, respectively) can be used as an important index to evaluate the poison tolerance of Pt catalysts in MOR. The I_f/I_b of the Pt nanostars and Pt nanodendrites were 1.01 and 0.92, respectively, which are higher than that of the carbon-supported Pt nanoparticles (0.87),[39] indicating their relatively good poison tolerance. Moreover, after 50 scan cycles, only 2.8% and 3.5% decrease in I_f/I_b ratio for Pt nanostars and Pt nanodendrites, respectively, were observed, implying they did not undergo serious deactivation during the continuous MOR.[40]

To investigate the thermal stability, the obtained Pt nanostars and Pt nanodendrities were annealed at various temperatures

(100 °C, 150 °C, and 200 °C) for several hours. After the thermal treatments, we investigated the CV shapes in H_2SO_4 solution. The typical CV curves for Pt were observed in both the samples. Even after the thermal treatment, the CV curves were not changed so much. The serious loss of specific surface areas was not confirmed, indicating good thermal stability.

The onset potentials of Pt nanostars and Pt nanodendrites (~ 0.26 V) negatively shift compared with that of Pt black (~ 0.42 V), facilitating Pt nanostars and Pt nanodendrites having lower potential for MOR at the same oxidation current density (see Figure S9b in the Supporting Information). In chronoamperometric investigations recorded at 0.6 V for 1800 s, Pt nanostars and Pt nanodendrites show higher mass current densities than Pt black during the entire testing time (see Figure S9c in the Supporting Information). All the investigations reveal that our Pt nanostars and Pt nanodendrites have excellent electrocatalytic activities for MOR. Considering their ultrafine particle sizes and dendritic structural features, the enhanced catalytic activities of the Pt nanostars and Pt nanodendrites might be ascribed to their sufficient active sites and excellent surface permeability in comparison with that of Pt black (see Figure S10 in the Supporting Information).

In summary, we successfully prepared two kinds of Pt nanoarchitecture (i.e., nanodendrites and nanostars) by a very simple method in high-yield at room temperature within 5 min from commercially available nonionic block copolymer aqueous solution. The present synthesis has a remarkable advantage in its simplicity for the synthesis of Pt nanocatalysts, in comparison with both traditionally thermal decomposition methods by using high boiling-point solvents and seed-mediated methods performed by two-step approaches. Pt nanodendrites and Pt nanostars not only improved the active Pt surface area but also showed superior electrochemical performance, which make them promising electrocatalysts for the future.

■ ASSOCIATED CONTENT

Ⓢ Supporting Information

Experimental details and additional characterization data. This material is available free of charge via the Internet at http://pubs.acs.org.

■ AUTHOR INFORMATION

Corresponding Author

*E-mail: YAMAUCHI.Yusuke@nims.go.jp.

Notes

The authors declare no competing financial interest.

■ REFERENCES

(1) (a) Guo, S. J.; Wang, E. K. *Nano Today* **2011**, *6*, 240. (b) Guo, S. J.; Dong, S. J.; Wang, E. K. *Chem. Commun.* **2010**, *46*, 1869. (c) Motokawa, S; Mohamedi, M; Momma, T; Shoji, S; Osaka, T. *Electrochemistry* **2005**, *73*, 346. (d) Tominaka, S.; Wu, C. W.; Kuroda, K.; Osaka, T. *J. Power Sources* **2009**, *195*, 2236.

(2) (a) Chen, A. C.; Holt-Hindle, P. *Chem. Rev.* **2010**, *110*, 3767. (b) Li, Y. M.; Somorjai, G. A. *Nano Lett.* **2010**, *10*, 2289. (c) Koenigsmann, C.; Wong, S. S. *Energy Environ. Sci.* **2011**, *4*, 1161.

(3) (a) Chen, J. Y.; Lim, B.; Lee, E. P.; Xia, Y. N. *Nano Today* **2009**, *4*, 81. (b) Xia, Y. N.; Xiong, Y. J.; Lim, B.; Skrabalak, S. E. *Angew. Chem., Int. Ed.* **2009**, *48*, 60.

(4) (a) Wang, C.; Daimon, H.; Lee, Y.; Kim, J.; Sun, S. H. *J. Am. Chem. Soc.* **2007**, *129*, 6974. (b) Ren, J. T.; Tilley, R. D. *J. Am. Chem. Soc.* **2007**, *129*, 3287.

(5) (a) Tsung, C. K.; Kuhn, J. N.; Huang, W. Y.; Aliaga, C.; Hung, L. I.; Somorjai, G. A.; Yang., P. D. *J. Am. Chem. Soc.* **2009**, *131*, 5816. (b) Wang, L.; Yamauchi, Y. *J. Am. Chem. Soc.* **2009**, *131*, 9152.

(6) Mostafa, S.; Behafarid, F.; Croy, J. R.; Ono, L. K.; Li, L.; Yang, J. C.; Frenkel, A. I.; Cuenya, B. R. *J. Am. Chem. Soc.* **2010**, *132*, 15714.

(7) Shao, M. H.; Peles, A.; Shoemaker, K. *Nano Lett.* **2011**, *11*, 3714.

(8) Komanicky, V.; Iddir, H.; Chang, K.; Menzel, A.; Karapetrov, G.; Hennessy, D.; Zapol, P.; You, H. *J. Am. Chem. Soc.* **2009**, *131*, 5732.

(9) Arenz, M.; Mayrhofer, K. J. J.; Stamenkovic, V.; Blizanac, B. B.; Tomoyuki, T.; Ross, P. N.; Markovic, N. M. *J. Am. Chem. Soc.* **2005**, *127*, 6819.

(10) (a) Qiao, B. T.; Wang, A. Q.; Yang, X. F.; Allard, L. F.; Jiang, Z.; Cui, Y. T.; Liu, J. Y.; Li, J.; Zhang, T. *Nat. Chem.* **2011**, *3*, 634. (b) Lee, H.; Habas, S. E.; Kweskin, S.; Butcher, D.; Somorjai, G. A.; Yang, P. D. *Angew. Chem., Int. Ed.* **2006**, *45*, 7824.

(11) Huang, X. Q.; Zhao, Z. P.; Fan, J. M.; Tan, Y. M.; Zheng., N. F. *J. Am. Chem. Soc.* **2011**, *133*, 4718.

(12) Yu, T.; Kim, D. Y.; Zhang, H.; Xia, Y. N. *Angew. Chem., Int. Ed.* **2011**, *50*, 2773.

(13) Peng, Z. M.; You, H. J.; Wu, J. B.; Yang, H. *Nano Lett.* **2010**, *10*, 1492.

(14) Takai, A.; Ataee-Esfahani, H.; Doi, Y.; Fuziwara, M.; Yamauchi, Y.; Kuroda, K. *Chem. Commun.* **2011**, *47*, 7701.

(15) Lim, S. I.; Ojea-Jimenez, I.; Varon, M.; Casals, E.; Arbiol, J.; Puntes, V. *Nano Lett.* **2010**, *10*, 964.

(16) Song, Y. J.; Garcia, R. M.; Dorin, R. M.; Wang, H. R.; Qiu, Y.; Shelnutt, J. A. *Angew. Chem., Int. Ed.* **2006**, *45*, 8126.

(17) (a) Sun, S. H.; Zhang, G. X.; Geng, D. S.; Chen, Y. G.; Li, R. Y.; Cai, M.; Sun, X. L. *Angew. Chem., Int. Ed.* **2011**, *50*, 422. (b) Wang, S. Y.; Jiang, S. P.; Wang, X.; Guo, J. *Electrochim. Acta* **2011**, *56*, 1563. (c) Zhou, W. P.; Li, M.; Koenigsmann, C.; Ma, C.; Wong, S. S.; Adzic, R. R. *Electrochim. Acta* **2011**, *56*, 9824. (d) Wu, B. H.; Zheng, N. F.; Fu, G. *Chem. Commun.* **2011**, *47*, 1039. (e) Kibsgaard, J.; Gorlin, Y.; Chen, Z. B.; Jaramillo, T. F. *J. Am. Chem. Soc.* **2012**, *134*, 7758. (f) Wang, H. J.; Wang, L.; Sato, T.; Sakamoto, Y.; Tominaka, S.; Miyasaka, K.; Miyamoto, N.; Nemoto, Y.; Terasaki, O.; Yamauchi, Y. *Chem. Mater.* **2012**, *24*, 1591.

(18) (a) Mankin, M. N.; Mazumder, V.; Sun, S. H. *Chem. Mater.* **2011**, *23*, 132. (b) Wang., L.; Yamauchi, Y. *Chem.—Eur. J.* **2011**, *17*, 8810. (c) Surendran, G.; Ramos, L.; Pansu, B.; Prouzet, E.; Beaunier, P.; Audonnet, F.; Remita, H. *Chem. Mater.* **2007**, *19*, 5045.

(19) (a) Gorzny, M. Ł.; Walton, A. S.; Evans, S. D. *Adv. Funct. Mater.* **2010**, *20*, 1295. (b) Yang, H. Z.; Zhang, J.; Sun, K.; Zou, S. Z.; Fang, J. Y. *Angew. Chem., Int. Ed.* **2010**, *49*, 6848.

(20) (a) Guo, S. J.; Zhang, S.; Sun, X. L.; Sun, S. H. *J. Am. Chem. Soc.* **2011**, *133*, 15354. (b) Bai, F.; Sun, Z. C.; Wu, H. M.; Haddad, R. E.; Xiao, X. Y.; Fan, H. Y. *Nano Lett.* **2011**, *11*, 3759. (c) Ye, Y. J.; Joo, J.; Lim, B.; Lee, J. *Chem.—Eur. J.* **2012**, *18*, 2797.

(21) (a) Shi, Y.; Wan, Y.; Zhao, D. *Chem. Soc. Rev.* **2011**, *40*, 3854. (b) Shi, Y.; Wan, Y.; Zhang, R.; Zhao, D. *Adv. Funct. Mater.* **2008**, *18*, 2436. (c) Sun, X.; Shi, Y.; Zhang, P.; Zheng, C.; Zheng, X.; Zhang, F.; Zhang, Y.; Guan, N.; Zhao, D.; Stucky, G. D. *J. Am. Chem. Soc.* **2011**, *133*, 14542.

(22) (a) Shin, H. J.; Ryoo, R.; Liu, Z.; Terasaki, O. *J. Am. Chem. Soc.* **2001**, *123*, 1246. (b) Wang, H. J.; Jeong, H. Y.; Imura, M.; Wang, L.; Radhakrishnan, L.; Fujita, N.; Castle, T.; Terasaki, O.; Yamauchi, Y. *J. Am. Chem. Soc.* **2011**, *133*, 14526.

(23) (a) Dag, Ö.; Alayoğlu, S.; Uysal, İ. *J. Phys. Chem. B* **2004**, *108*, 8439. (b) Dag, Ö.; Alayoğlu, S.; Tura, C.; Çelik, Ö. *Chem. Mater.* **2003**, *15*, 2711. (c) Türker, Y.; Dag, Ö. *J. Mater. Chem.* **2008**, *18*, 3467.

(24) (a) Attard, G. S.; Bartlett, P. N.; Coleman, N. R. B.; Elliott, J. M.; Owen, J. R.; Wang, J. H. *Science* **1997**, *278*, 838. (b) Yamauchi, Y.; Kuroda, K. *Chem. Asian J.* **2008**, *3*, 664.

(25) Lim, B.; Xia, Y. N. *Angew. Chem., Int. Ed.* **2011**, *50*, 76.

(26) Mohanty, A.; Garg, N.; Jin, R. C. *Angew. Chem., Int. Ed.* **2010**, *49*, 4962.

(27) Lin, Z. H.; Lin, M. H.; Chang, H. T. *Chem.-Eur. J* **2009**, *15*, 4656.

(28) Teng, X. W.; Liang, X. Y.; Maksimuk, S.; Yang, H. *Small* **2006**, *2*, 249.
(29) Peng, Z. M.; Yang, H. *Nano Today* **2009**, *4*, 143.
(30) Cheong, S.; Watt, J.; Ingham, B.; Toney, M. F.; Tilley, R. D. *J. Am. Chem. Soc.* **2009**, *131*, 14590.
(31) Zhong, X. H.; Feng, Y. Y.; Lieberwirth, I.; Knoll, W. *Chem. Mater.* **2006**, *18*, 2468.
(32) Shen, Q. M.; Jiang, L. P; Zhang, H.; Min, Q. H.; Hou, W. H.; Zhu, J. J. *J. Phys. Chem. C* **2008**, *112*, 16385.
(33) Mandal, S.; Sathish, M.; Saravanan, G.; Datta, K. K. R.; Ji, Q. M.; Hill, J. P.; Abe, H.; Honma, I.; Ariga, K. *J. Am. Chem. Soc.* **2010**, *132*, 14415.
(34) Mahmoud, M. A.; Tabor, C. E.; El-Sayed, M. A.; Ding, Y.; Wang, Z. L. *J. Am. Chem. Soc.* **2008**, *130*, 4590.
(35) Zhou, Z. Y.; Huang, Z. Z.; Chen, D. J.; Wang, Q.; Tian, N.; Sun, S. G. *Angew. Chem., Int. Ed.* **2010**, *49*, 411.
(36) Tian, N.; Zhou, Z. Y.; Sun, S. G.; Ding, Y.; Wang, Z. L. *Science* **2007**, *316*, 732.
(37) Wu, B.; Hu, D.; Kuang, Y.; Liu, B.; Zhang, X.; Chen, J. *Angew. Chem., Int. Ed.* **2009**, *48*, 4751.
(38) Sun, S. H.; Zhang, G. X.; Geng, D. S.; Chen, Y. G.; Banis, M. N.; Li, R. Y.; Cai, M.; Sun, X. L. *Chem.—Eur. J.* **2010**, *16*, 829.
(39) Liu, Z. L.; Ling, X. Y.; Su, X. D.; Lee, J. Y. *J. Phys. Chem. B* **2004**, *108*, 8234.
(40) Bai, L. T.; Zhu, H. Z.; Thrasher, J. S.; Street., S. C. *ACS Appl. Mater. Interfaces* **2009**, *1*, 2304.